

CONF-970455--2

**CHARACTERISTICS OF A MULTICOMPONENT Nb-Ti-Al ALLOY
VIA INDUSTRIAL-SCALE PRACTICE**

V. K. Sikka
Metals and Ceramics Division
Oak Ridge National Laboratory
P.O. Box 2008
Oak Ridge, Tennessee 37831-6083

and

E. A. Loria
Reference Metals Company, Inc.
1000 Old Pond Road
Bridgeville, Pennsylvania 15017-0217

RECEIVED
MAY 16 1997
OSTI

4th International Conference on High Temperature Intermetallics, San Diego, CA,
April 27-May 1, 1997.

KEYWORDS

1. Niobium
2. Tensile testing
3. Vacuum testing
4. Interstitial content
5. Multicomponent
6. Scanning microscopy
7. Fracture surfaces
8. Oxygen embrittlement
9. Nb-Ti alloys
10. Nickel-base superalloys

MASTER

DISTRIBUTION OF THIS DOCUMENT IS UNLIMITED

Um

DISCLAIMER

This report was prepared as an account of work sponsored by an agency of the United States Government. Neither the United States Government nor any agency thereof, nor any of their employees, make any warranty, express or implied, or assumes any legal liability or responsibility for the accuracy, completeness, or usefulness of any information, apparatus, product, or process disclosed, or represents that its use would not infringe privately owned rights. Reference herein to any specific commercial product, process, or service by trade name, trademark, manufacturer, or otherwise does not necessarily constitute or imply its endorsement, recommendation, or favoring by the United States Government or any agency thereof. The views and opinions of authors expressed herein do not necessarily state or reflect those of the United States Government or any agency thereof.

DISCLAIMER

Portions of this document may be illegible in electronic image products. Images are produced from the best available original document.

CHARACTERISTICS OF A MULTICOMPONENT Nb-Ti-Al ALLOY VIA INDUSTRIAL-SCALE PRACTICE

V. K. Sikka
Metals and Ceramics Division
Oak Ridge National Laboratory[†]
P.O. Box 2008
Oak Ridge, Tennessee 37831-6083

and

E. A. Loria
Reference Metals Company, Inc.
1000 Old Pond Road
Bridgeville, Pennsylvania 15017-0217

ABSTRACT

Within the spectrum of advanced intermetallic materials, an alloy containing 44Nb-35Ti-6Al-5Cr-8V-1W-0.5Mo-0.3Hf (at. %) was investigated in the industrial-scale produced condition. The alloy was tensile tested in air from room temperature to 1000°C and in vacuum at 750 and 850°C. Results of this study have shown that the alloy can be commercially produced and has adequate ductility for its secondary processing even at an oxygen level of 1160 wppm. The alloy has room temperature ductility of 16% and superplastic elongation of 244% at 1000°C. This alloy shows low intermediate temperature (600-850°C) ductility when tested in air. The vacuum testing revealed that the low ductility is associated within oxygen embrittlement phenomenon. It is expected that such an embrittlement can be taken care of by an oxidation resistant coating. The alloy also possesses superior strength to similar alloys in this class. Results of this investigation suggest a strong potential for consideration of this alloy to exceed the useful temperature range of nickel-base superalloys.

[†]Managed by the U.S. Department of Energy under contract DE-AC05-96OR22464 with Lockheed Martin Energy Research Corp.

The submitted manuscript has been authored by a contractor of the U.S. Government under contract No. DE-AC05-96OR22464. Accordingly, the U.S. Government retains a nonexclusive, royalty-free license to publish or reproduce the published form of this contribution, or allow others to do so, for U.S. Government purposes.

INTRODUCTION

The need for new non-nickel-based superalloys for hot sections of aircraft jet engines and aerospace vehicles has focused attention on certain alloys that exist in the Nb-Ti-Al system. Within the spectrum of advanced intermetallic materials, these alloys have been categorized as ductile systems [1]. The alloys are bcc solid solutions, have higher melting points than nickel-based alloys, and can be tailored to vary their melting point and density. This has been shown by the performance of the 40Nb-40Ti-10Al-10Cr alloy [2] as well as the compositional limits of Nb-Ti alloys, which provide ductile room-temperature behavior and improved oxidation resistance [3].

The Nb-Ti base can be substantially alloyed with aluminum, hafnium, chromium, and other elements to provide higher strength with ductility. Increased yield strength as a function of temperature has been shown [4] for Alloy 3899-4, which contains 41Nb-37Ti-5Al-5Cr-5V-5Hf-0.5Zr-0.2Sn (at. %). This paper presents the introductory properties for another alloy containing 44Nb-35Ti-6Al-5Cr-8V-1W-0.5Mo-0.3Hf (at. %) which, instead of being evaluated based upon small quantities derived from laboratory-scale heats, has been produced via industrial-scale operations.

MATERIAL AND PROCEDURE

Alloy preparation involved powder metallurgy technology via mixing and pressing commercially available materials into disks at Oremet and double-plasma-arc cold-hearth melting at Retech to produce an ingot measuring 15.3 cm diam by 61.0 cm length and weighing 73.5 kg. After surface machining, the ingot was canned in 19-mm-thick type 304 stainless steel and extruded in the Amax 5000-ton press, using a soaking temperature of 1100°C for 2.5 h. The 5.3:1 reduction produced an extrusion of 8.13 cm diam and 305 cm length. Then, an appropriate length was reextruded to 25.4 mm diam on the Oak Ridge National Laboratory's 1250-ton press and cold swaged to 15.9 mm diam. Other details on chemical segregation via microprobe analysis both before and after ingot homogenization have been presented [5].

This end-product, with the adhering stainless rim, was vacuum annealed at 1100°C for 1 h, resulting in a recrystallized grain size of 22 to 25 μm (ASTM 8), and the 12.7-mm-diam specimens were machined with a

gauge diam of 6.35 mm and length for 30 min of 31.7 mm (overall length is 82.6 mm). Tensile tests were conducted at room temperature and at 600 to 1000°C in air. The time to equilibrate the specimens to the test temperature in air was around 30 min, and the strain rate in all cases was 3×10^{-3} /s. Scanning electron microscopy (SEM) was employed in the examination of these specimens.

RESULTS AND DISCUSSION

The interstitial element content of the alloy obtained at various stages of processing is given in Table 1. It should be recognized that these results occurred from the use of alloying materials having the lowest content of these elements commercially available in quantity at reasonable cost for this production feasibility study. Under these circumstances, the oxygen content of 1160 wppm is significantly higher than has been obtained in the laboratory-scale heats studied to date. For example, Alloy 3899-4 contained 500 wppm oxygen, and the range of oxygen content in other small heats has been 400 to 600 wppm. It is well known that the deformation behavior of Nb-Ti alloys is sensitive to interstitial impurities such as oxygen, and this study is the first one to present positive results at 1160-wppm oxygen content.

As shown in Table 2, an optimum combination of 1107 MPa yield strength and 16% elongation (51% reduction of area) was obtained at room temperature which are the highest values obtained in a comparison of the tensile properties with existing Nb-Ti alloys. The room-temperature ductility controls alloy design since it is a practical consideration that cannot be ignored in developing alloys for application in real systems. Another important result was the highest yield strength of 280 MPa and (unexpected) elongation of 244% when testing in air at 1000°C. Superplastic elongation and high yield strength under these conditions would enhance isothermal forging of integral shapes. In comparison, 0.76-mm-thick sheet of Alloy 3899-4 has 952 MPa yield strength and 12% elongation at room temperature and 179 MPa yield strength with 59% elongation when tested in vacuum at 1000°C [ref. 4].

The scanning electron microscope (SEM) photographs of the tensile tested specimens at room temperature with 16.2% elongation and with superplastic elongation of 244% at 1000°C are shown in Fig. 1. This figure shows the classical cup and cone ductile fracture at room temperature and a greatly elongated and a

small fracture cross section for the 1000°C tested specimen. The dramatic difference in fracture cross sections for the room temperature and 1000°C tested specimens are shown in Fig. 2. The higher magnification micrographs of the room temperature and 1000°C specimens are compared in Fig. 3. These micrographs show the ductile tearing fracture mode for the room temperature tested specimen. The fracture surface of the 1000°C specimen also shows ductile fracture but the fracture surface is oxidized from being exposed to 1000°C in the test furnace after fracture. The surface of specimen tested in air at 1000°C is also oxidized, Fig. 1(b), and in the absence of this oxidation the specimen would have elongated even more than 244% observed here.

As seen in Table 2, there is an intermediate temperature range of 700 to 850°C where testing in air under the hold time of 30 min to equilibrate the specimens to the test temperature resulted in only 2% elongation. Oxygen penetration embrittlement in air was the cause and attributed to the changing degree of surface protection provided by the alloying elements. The 2% elongation in air at 750 and 800°C would not eliminate the alloy from application because it would be coated (surface protected). The effect of oxygen penetration on ductility was evaluated by conducting tensile tests in vacuum at 750 and 800°C. The tests in vacuum (Table 2) show that the low ductility values in air are related to embrittlement caused by oxygen penetration.

The dramatic difference of oxygen related embrittlement is shown in the SEM photographs of the specimens tensile tested in air and vacuum at 750 and 850°C in Fig. 4. The specimen tested in air at 750°C shows a totally intergranular fracture as opposed to nearly 100% ductile tearing for specimen tested in vacuum at the same temperature shown in Fig. 5. The specimen tested in air at 850°C also has a 100% intergranular fracture as shown in Fig. 6. The testing in vacuum at 850°C produces approximately 75% ductile fracture (Fig. 6) as opposed to 100% for 750°C. This suggests that the vacuum used in our testing was not adequate to completely eliminate oxygen related embrittlement at 850°C. Photomicrographs of Figs. 4-6 suggest that oxygen penetrated across the entire specimen diameter during testing in air at 750 and 850°C and is limited to no penetration in vacuum at 750°C and to few grains depth for testing in vacuum at 850°C. The specimens tested in air at 600°C also showed intergranular fracture, but with scattered ductile tearing. This implies that the oxygen related embrittlement phenomenon started below 600°C. The exact temperature for the initiation of such embrittlement is not known because no testing was done between room temperature and 600°C.

The 0.2% yield and ultimate tensile strength properties of the alloy of this study (44Nb-35Ti-6Al-5Cr-8V-1W-0.5Mo-0.3Hf) are compared with other Nb-base alloys in Figs. 7 and 8. These figures show that the alloy of this study has higher tensile strength properties than other alloys for the test temperature range for which the data are available. The data in Table 2 shows that the alloy also has good ductility at room temperature and 1000°C. The poor ductility in the intermediate temperature is a result of oxygen embrittlement which can be reduced through the use of proper coatings.

CONCLUSIONS

An alloy within the spectrum of advanced intermetallic materials containing 44Nb-35Ti-6Al-5Cr-8V-1W-0.5Mo-0.3Hf (at. %) was investigated in the industrial scale produced condition. The alloy was tensile tested in air from room temperature to 1000°C. It was also tested in vacuum at 750 and 850°C to illustrate that the low ductility in the intermediate range is caused by oxygen embrittlement in air. Tensile tested specimens were examined by scanning electron microscope analysis. The following conclusions are possible from this work:

1. The alloy can be produced on an industrial scale.
2. The alloy was processable with adequate ductility at room temperature, even with an oxygen content of 1160 wppm.
3. The alloy shows good ductility of 16% at room temperature and superplastic elongation of 244% at 1000°C.
4. The low ductility in air tested specimens between 750 and 850°C was shown to be associated with intergranular fracture caused by oxygen embrittlement. This was confirmed by a change of fracture mode to ductile dimple rupture for tests in vacuum at the two temperatures.
5. The alloy also shows superior strength to other alloys in the same class.

ACKNOWLEDGMENTS

The authors wish to thank C. Randy Howell for testing and data analyses, E. K. Ohriner and G. M. Goodwin for paper review, and Glenda Carter for preparing the manuscript.

REFERENCES

1. D.M. Dimiduk, M.G. Mendiratta, and P.R. Subramanian, Development Approaches for Advanced Intermetallic Materials-Historical Perspective and Selected Successes, in *Structural Intermetallics*, Ed. R. Darolia et al., pub. The Minerals, Metals, and Materials Society, Warrendale, PA, 1993, p619-630.
2. V.K. Sikka, S. Viswanathan, and E.A. Loria, Processing and Properties of Nb-Ti-Based-Alloys, in *Superalloys*, Ed. S.D. Antolovich et al., pub. The Minerals, Metals, and Materials Society, Warrendale, PA, 1992, p423-434.
3. M.R. Jackson and K.D. Jones, Mechanical Behavior of Nb-Ti-Based-Alloys, in *Refractory Metals Extraction, Processing and Applications*, Ed. K.C. Liddell et al., pub. The Minerals, Metals, and Materials Society, Warrendale, PA, 1991, p311-320.
4. M.R. Jackson, Ductile Low-Density Alloys Based on Niobium, in *Tungsten and Refractory Metals*, Ed. A. Bose, Pub. Metal Powder Industries Federation, Princeton, NJ, 1994, p657-664.
5. E.A. Loria, T. Carneiro, and H. Stuart, Processing Capability of Structural Intermetallics and Nb-Ti-Al Alloys via Plasma Arc Melting, in *Structural Intermetallics*, Ed. R. Darolia et al., pub. The Minerals, Metals, and Materials Society, Warrendale, PA, 1993, p699-706.

CAPTIONS

- Fig. 1. Scanning electron microscope (SEM) photographs of specimens tensile tested in air at (a) room temperature and (b) 1000°C.
- Fig. 2. Scanning electron microscope micrographs of fracture surfaces of specimens tested in air at (a) room temperature and (b) 1000°C. Note the significant difference in fracture cross section between the two specimens.
- Fig. 3. Scanning electron microscope micrographs of fracture surfaces of specimens tested in air at (a) and (b) room temperature and (c) and (d) at 1000°C.
- Fig. 4. Scanning electron microscope photographs of broken tensile specimens tested at 750°C in (a) air and (b) vacuum and at 850°C in (c) air and (d) vacuum. Note the significant improvement in ductility of specimens tested in vacuum.
- Fig. 5. Scanning electron microscope micrographs of fracture surfaces of specimens tensile tested at 750°C in air (a) low magnification, (b) high magnification and tested in vacuum (c) low magnification and (d) high magnification. Note the change from intergranular fracture in air tested to ductile dimple fracture in vacuum tested specimen.
- Fig. 6. The SEM micrographs of fracture surfaces of specimens tensile tested at 850°C in air (a) low magnification and (b) high magnification and tested in vacuum (c) low magnification and (d) high magnification. Note the changes from 100% intergranular fracture in air tested to 75% ductile dimple fracture in vacuum tested specimen.
- Fig. 7. Comparison of yield strength of B2 alloy, 44Nb-35Ti-6Al-5Cr-8V-1W-0.5Mo-0.3Hf with alloys in the same class. A = 40Nb-40Ti-10Al-10Cr, C = Alloy 3899-4, 41Nb-37Ti-5Al-5Cr-5V-5Hf-0.5Zr-0.2Sn, D = 45Nb-41Ti-12.5Al-1.5Mo. All of the compositions are in atomic percent.
- Fig. 8. Comparison of ultimate tensile strength of B2 alloy, 44Nb-35Ti-6Al-5Cr-8V-1W-0.5Mo-0.3Hf with alloys in the same class. A = 40Nb-40Ti-10Al-10Cr, C = Alloy 3899-4, 41Nb-37Ti-5Al-5Cr-5V-5Hf-0.5Zr-0.2Sn, D = 45Nb-41Ti-12.5Al-1.5Mo. All of the compositions are in atomic percent.

Table 1. Interstitial content of multicomponent
Nb-Ti-Al alloy

Product ^a	Weight percent			
	C	O	N	H
Ingot	0.0600	0.1450	0.010	0.003
Round A	0.0534	0.1200	0.0063	0.002
Round B	0.0600	0.1160	0.010	0.003

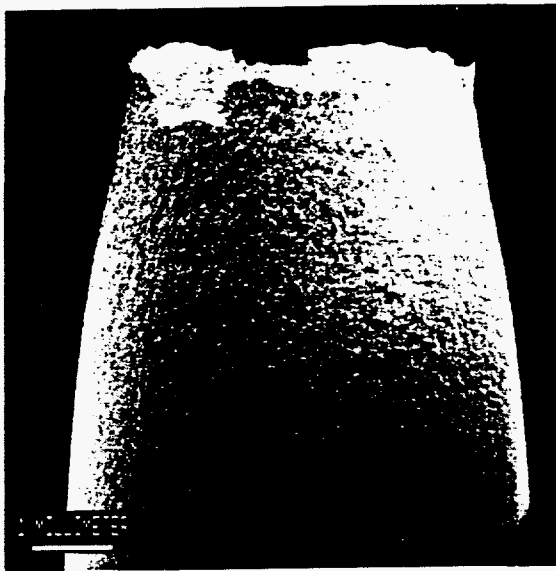
^aAverage value from 6-in.-diam ingot cross section, then individual values for extruded round A of 3 in. diam, and reextruded and then swaged round B of 0.5 in. diam.

Table 2. Tensile properties^a of multicomponent Nb-Ti alloy^bB2
 [44Nb-35Ti-6Al-5Cr-8V-1W-0.5Mo-0.3Hf (at%)]

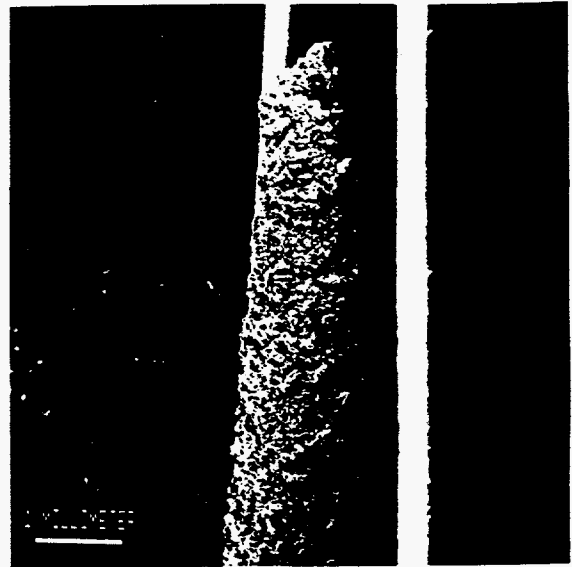
Test temperature (°C)	Yield strength		Ultimate strength		Total elongation (%)	Reduction of area (%)
	MPa	ksi	MPa	ksi		
Conducted in air						
23	1107	160.4	1117	162.0	16.2	50.7
600	668	96.9	841	121.9	8.4	9.8
750	627	90.7	669	96.9	1.8	1.0
800	582	84.3	612	88.7	2.1	2.0
850	544	78.9	551	79.9	4.8	4.3
1000	280	40.6	280	40.6	244.3	96.8
Conducted in vacuum						
750	595	86.3	681	98.7	26.8	59.9
850	539	78.2	542	78.6	36.0	60.9

^aTensile testing at a strain rate of 3×10^{-3} /s.

^bAs recrystallized vacuum heat treatment of 0.5-in.-diam bar at 1100°C for 1 h.

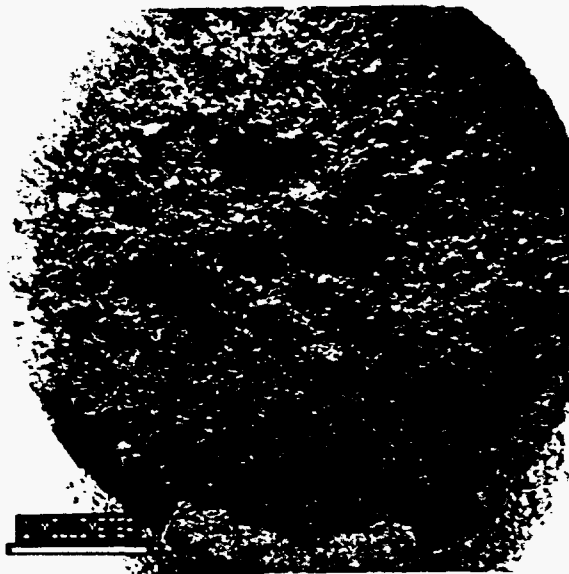


(a)

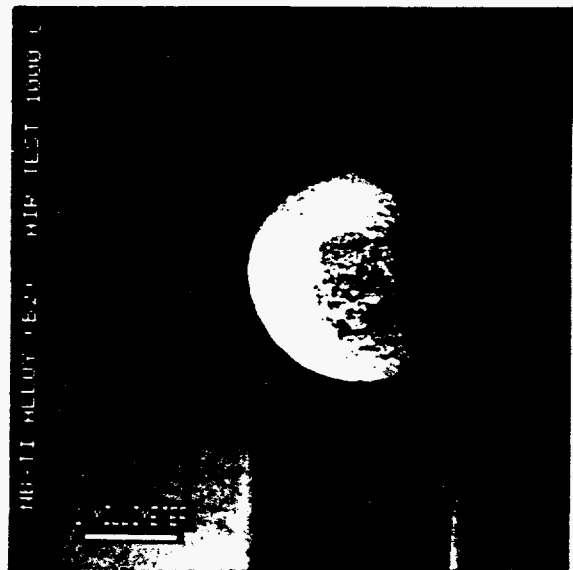


(b)

Fig. 1. Scanning electron microscope (SEM) photographs of specimens tensile tested in air at (a) room temperature and (b) 1000°C.

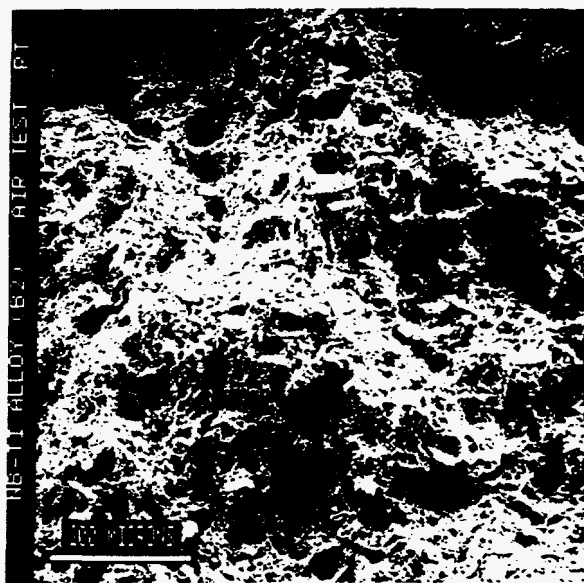


(a)

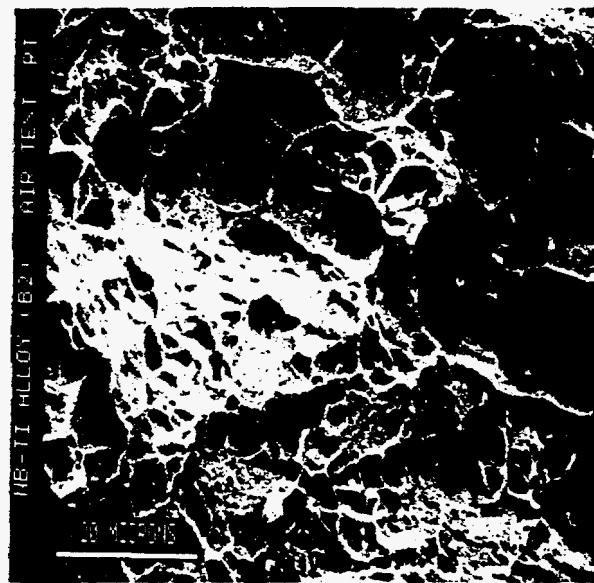


(b)

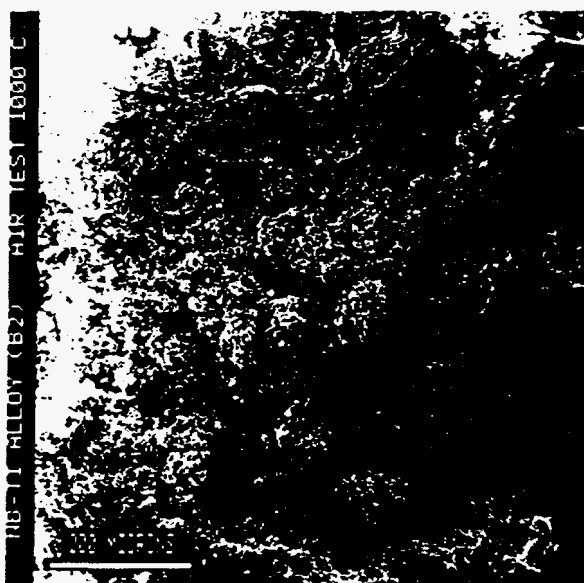
Fig. 2. Scanning electron microscope micrographs of fracture surfaces of specimens tested in air at (a) room temperature and (b) 1000°C. Note the significant difference in fracture cross section between the two specimens.



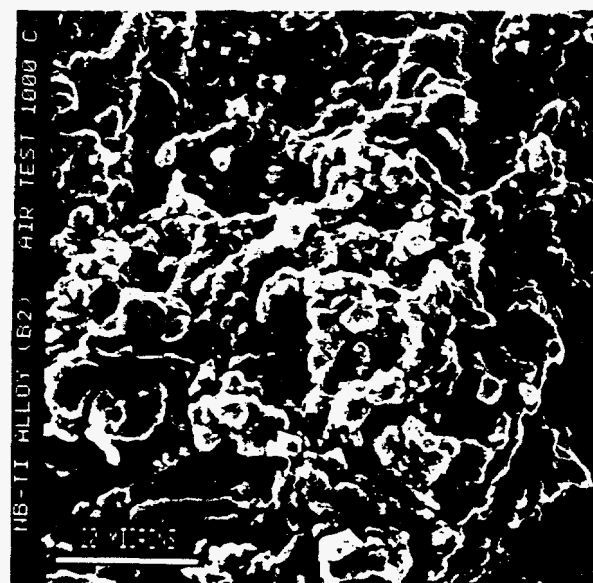
(a)



(b)



(c)



(d)

Fig. 3. Scanning electron microscope micrographs of fracture surfaces of specimens tested in air at (a) and (b) room temperature and (c) and (d) at 1000°C.

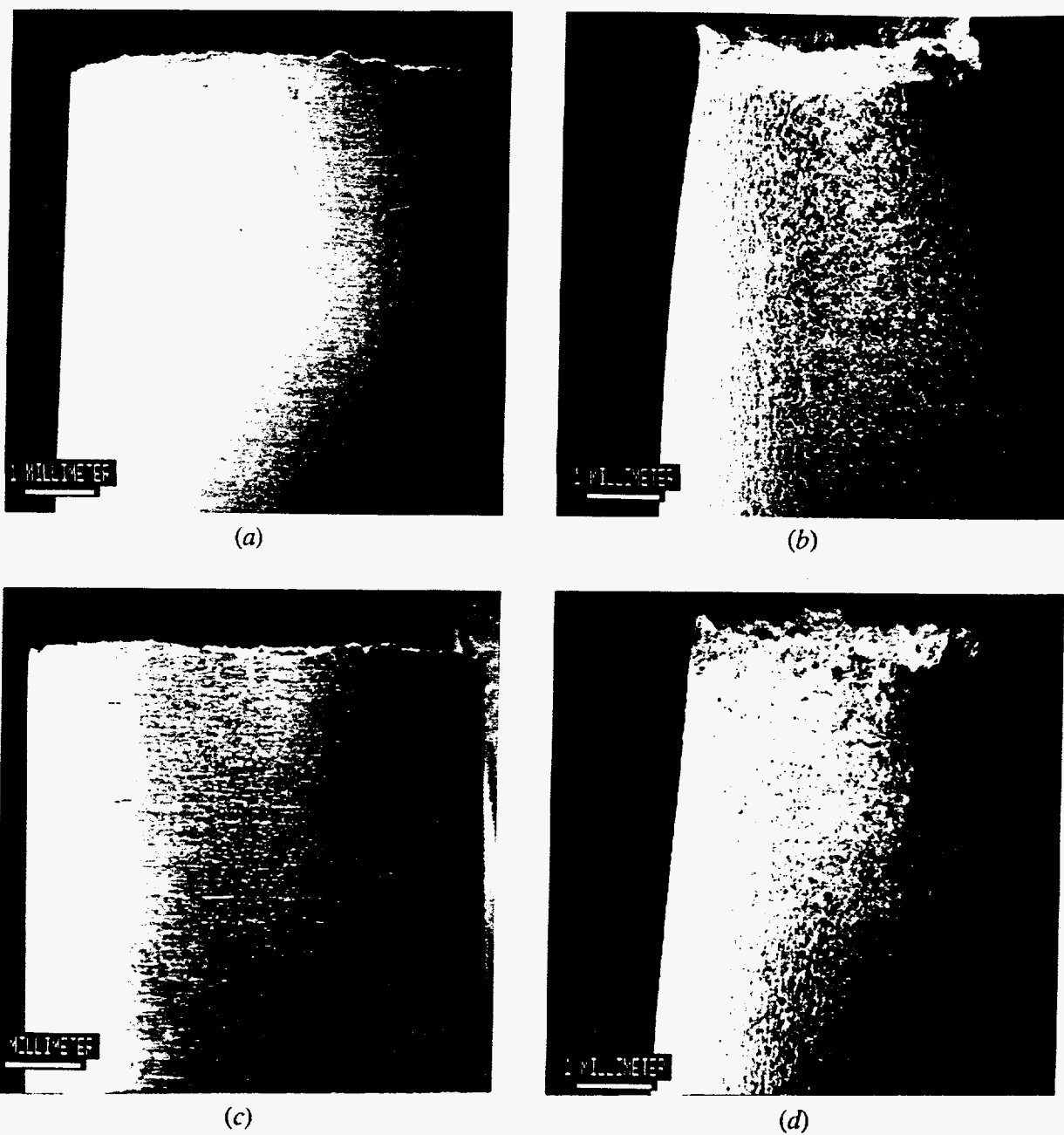
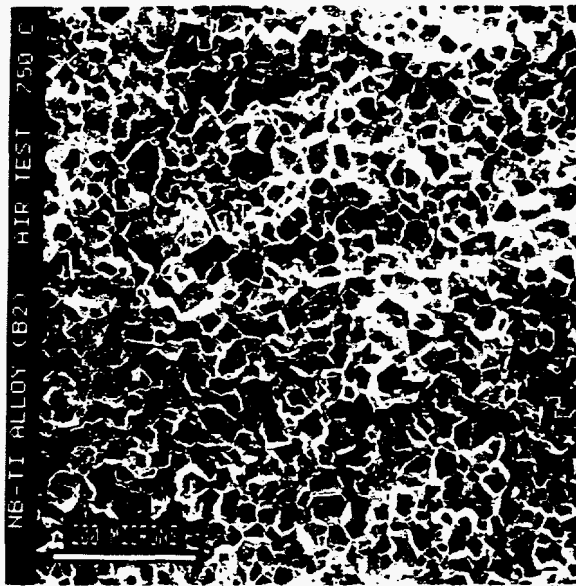
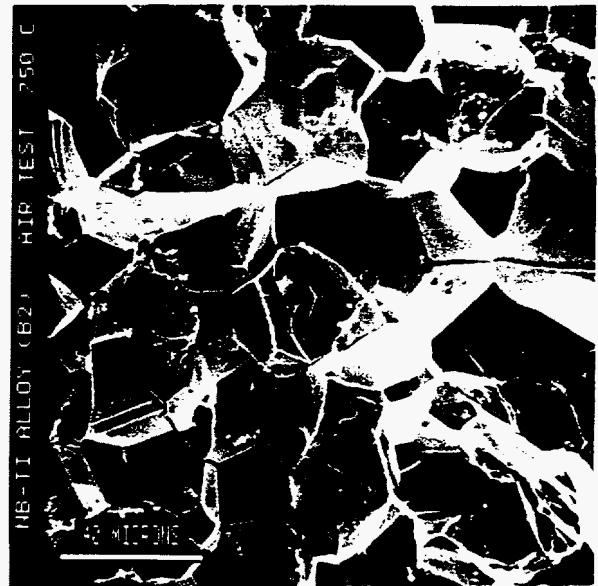


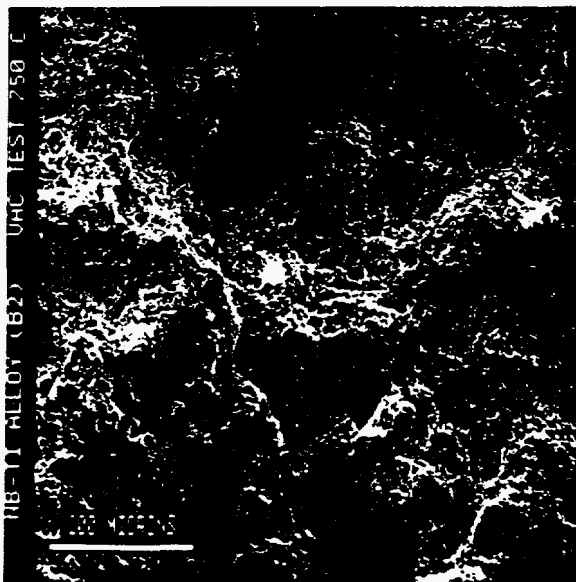
Fig. 4. Scanning electron microscope photographs of broken tensile specimens tested at 750°C in (a) air and (b) vacuum and at 850°C in (c) air and (d) vacuum. Note the significant improvement in ductility of specimens tested in vacuum.



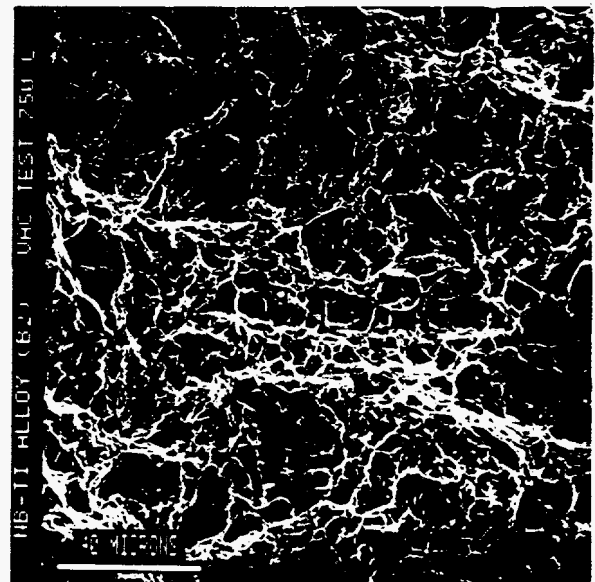
(a)



(b)

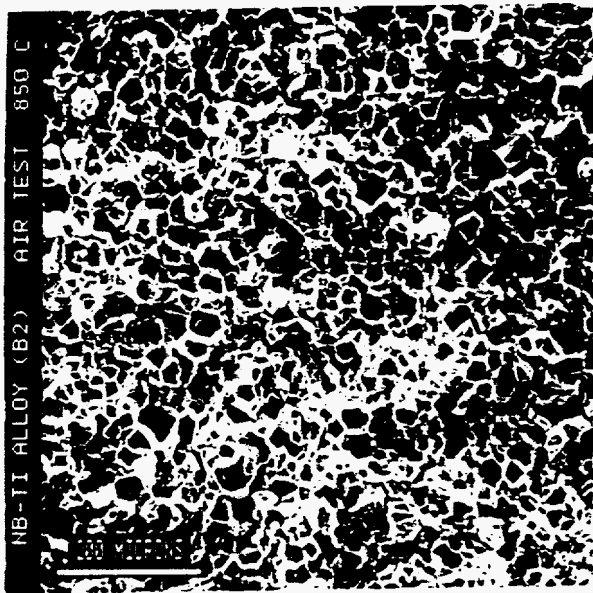


(c)

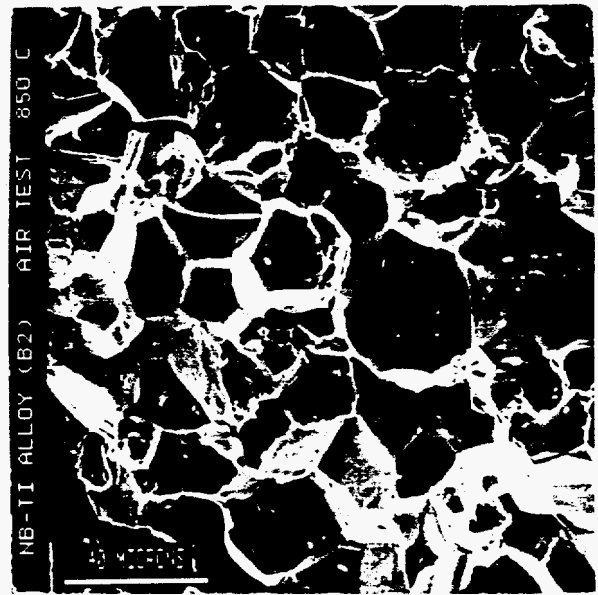


(d)

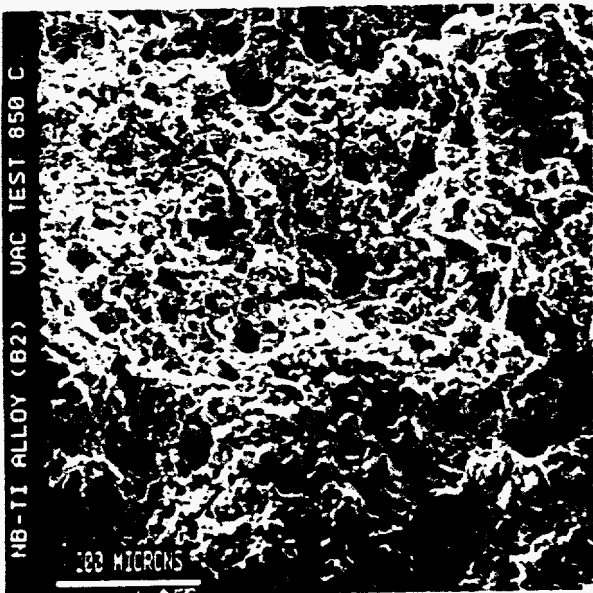
Fig. 5. Scanning electron microscope micrographs of fracture surfaces of specimens tensile tested at 750°C in air (a) low magnification, (b) high magnification and tested in vacuum (c) low magnification and (d) high magnification. Note the change from intergranular fracture in air tested to ductile dimple fracture in vacuum tested specimen.



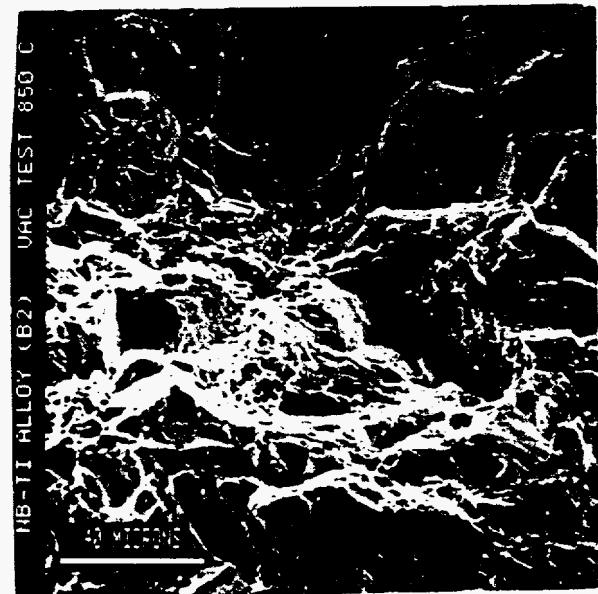
(a)



(b)



(c)



(d)

Fig. 6. Scanning electron microscope micrographs of fracture surfaces of specimens tensile tested at 850°C in air (a) low magnification and (b) high magnification and tested in vacuum (c) low magnification and (d) high magnification. Note the changes from 100% intergranular fracture in air tested to 75% ductile dimple fracture in vacuum tested specimen.

Tensile Properties

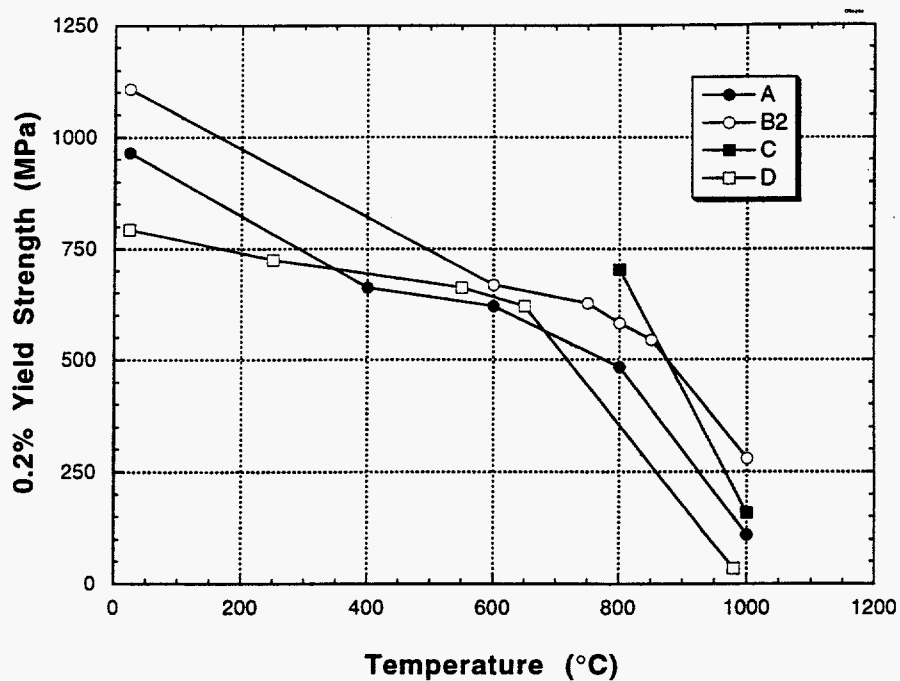


Fig. 7. Comparison of yield strength of B2 alloy, 44Nb-35Ti-6Al-5Cr-8V-1W-0.5Mo-0.3Hf with alloys in the same class. A = 40Nb-40Ti-10Al-10Cr, C = Alloy 3899-4, 41Nb-37Ti-5Al-5Cr-5V-5Hf-0.5Zr-0.2Sn, D = 45Nb-41Ti-12.5Al-1.5Mo. All of the compositions are in atomic percent.

Tensile Properties

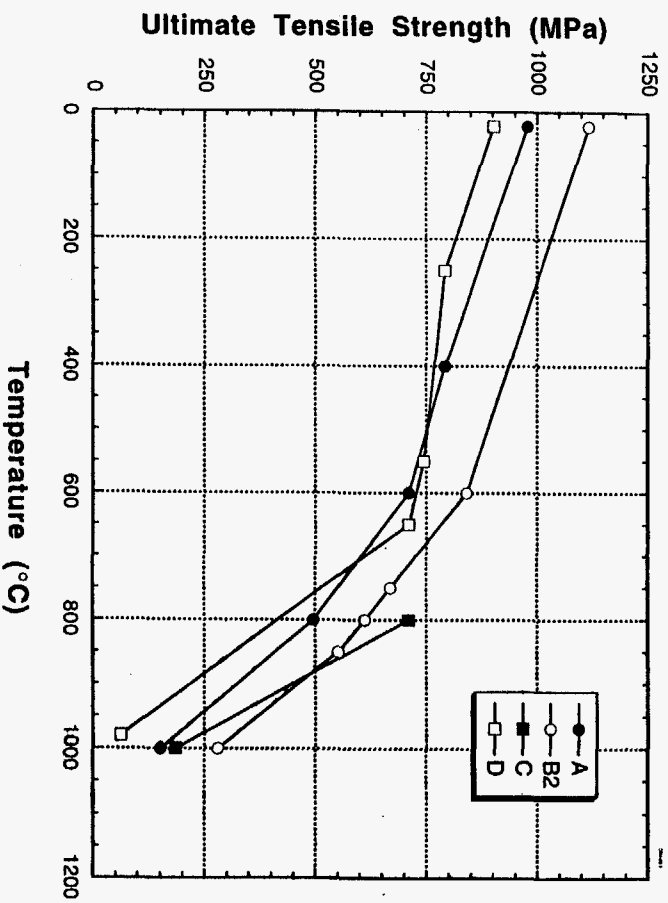


Fig. 8. Comparison of ultimate tensile strength of B2 alloy, 44Nb-35Ti-6Al-5Cr-8V-1W-0.5Mo-0.3Hf with alloys in the same class. A = 40Nb-40Ti-10Al-10Cr, C = Alloy 3899-4, 41Nb-37Ti-5Al-5Cr-5V-5Hf-0.5Zr-0.2Sn, D = 45Nb-41Ti-12.5Al-1.5Mo. All of the compositions are in atomic percent.